Res Mechanica **23** (1988) 137–160

A Review of Experimental Observations and Theoretical Models of Dislocation Cells and Subgrains

Robert J. Amodeo and Nasr M. Ghoniem

Mechanical, Aerospace and Nuclear Engineering Department,
University of California Los Angeles, Los Angeles, California 90024, USA

ABSTRACT

The formation of dislocation cells and subgrain structures is of great significance to the understanding of high-temperature deformation of many solids. Experimental observations on dislocation patterns, and in particular cellular structures, are reviewed. The basic features of such structures are discussed, and the conditions allowing dislocation patterning behavior are described. Theoretical formulations that attempt to model this phenomenon are reviewed, with emphasis on recent dynamical computer simulations.

1 INTRODUCTION

In the last two decades, much attention has been given to studying the phenomenon of dislocation cell formation in metals and other materials. The simplest understanding of this process is that, above a specific temperature, application of stress to a material leads to the formation of these structures. Below this temperature, dislocations are more or less homogeneously distributed throughout the medium. Cell formation appears to be a critical phenomenon, similar to a phase transition, in which the system state transforms from a condition of disorder to a condition of order.

Figure 1 is a graphical description of the phenomenon which occurs when the critical value of this temperature is achieved.[1] Application of stress to a material at lower temperatures produces a stress–strain curve in which the stress rises steadily as the material deforms, and then

Res Mechanica 0143-0084/88/$03·50

70

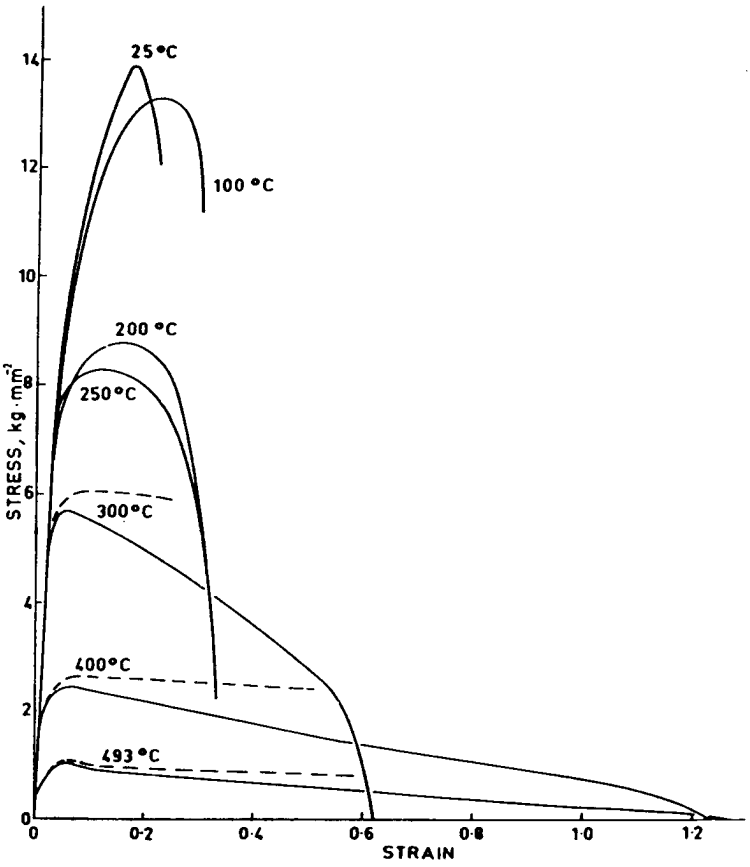

Fig. 1. Stress–strain diagram for aluminum (from Miekk-oja and Lindroos[1]).

reaches a maximum point, the ultimate tensile strength. After this point, the material weakens and reaches a point at which further straining of the material causes it to rupture. But above a certain temperature,[1] the material achieves a constant value of strength upon increased straining of the material. This behavior is attributed to the formation of dislocation cellular structures.

The formation of cells is generally considered to be a higher temperature phenomenon, associated with processes such as creep[2] and hot working.[3] The structural integrity of the material is altered with the presence of dislocation cells. Upon deformation, the matrix becomes strewn with dislocations produced by Frank–Read multiplication processes. After the dislocation cells crystallize, the material under stress enters secondary creep, and further deformation occurs at a constant value of strain rate.

There exist many scenarios in which materials are exposed to high

temperatures while being subjected to considerable stresses. Examples include the operation of fusion reactor first walls at high temperatures, the exposure of aircraft parts to high temperatures, and the effect of upper atmospheric conditions on spacecraft parts, just to name a few. Even at intermediate temperatures,[4] dislocation structural transformation occurs, and hence it is important to be able to predict when and under what conditions this transformation takes place. The process of dislocation cell formation is determined by the nature of the structure of the material. In particular, the crystal structure and alloy type influence the rate of dislocation interactions, which ultimately controls the rate of cell formation.

Cells and subgrains can be responsible for the phenomenon of steady–state creep.[5] The actual process of cell formation and the overall creep process, however, are coupled in a manner that does not necessarily lead to a clear understanding of deformation. Although cells are present at the onset and during steady–state creep, they are believed to be formed during the primary transient stage.[4] In the literature, however, cell structures have mostly been studied post-stage I, after the coarsening process to subgrain structures has begun to occur. Very little work has been done to demonstrate the *in-situ* process of cell formation.

It is the intent of this work to review the general characteristics of dislocation cells and subgrains. Information will be mostly based upon experimental observations. Theoretical considerations will also be addressed. Finally, a model designed to study the process of cell formation will be presented, in an attempt to run a 'computer experiment' to fill in the gap between initial deformation and the completion of dislocation cell formation.

2 GENERAL CHARACTERISTICS OF DISLOCATION CELLS/SUBGRAINS

The dislocation cell structure can be described as a two-dimensional honeycomb-like configuration in which there are regions of high dislocation density, the cell walls, and low dislocation density, the region in between the walls. A subgrain is a structure resembling a grain, which is formed by the condensation of the sub-boundaries of dislocation cells into long thin boundaries. Direct observation of both of these structures has been reported in several papers for many different materials.[6–13] Figure 2 is a schematic representation of the evolution of the microstructure of a material at various stages of

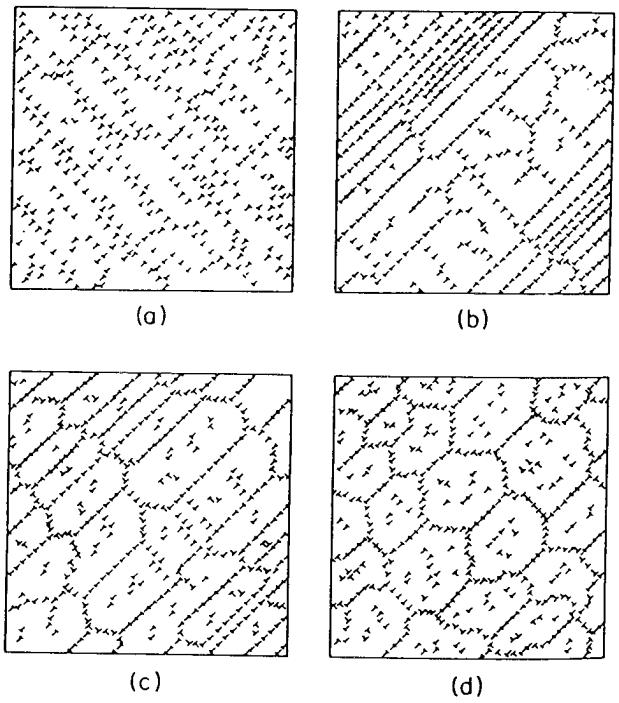

Fig. 2. Evolution of cellular microstructure during creep (from Takeuchi and Argon[2]).

straining (from Ref. 2). It represents a general picture of the progression of dislocation cell and subgrain formation based on several experiments.[14–16] Takeuchi and Argon[2] have summarized the sequence of transgression of substructure formation upon deformation as follows:

(a) Initially, the dislocations are strewn randomly through matrix.
(b) They then form the homogeneous 'cell-like' structures in which the walls of the cells are of finite thickness, and comprise many dislocations.
(c) Heterogeneous structures begin to form: subgrains which result from elongation of cells, coalescence of cells, and recovery within the cell walls.
(d) Eventually a homogeneous equiaxed structure of subgrains forms.

Dislocation cells and subgrains are most likely to form in pure metals and class II alloys. In both these materials, the deformation characteristic (elongation versus stress) follows a stress dependence of exponent 5.[17] It has been shown[16] that the conditions characteristic of

high-temperature creep are most conducive to the formation of equiaxed cellular type structures. In this study it was found that α-phase iron forms banded structures under conditions of high stress and low temperature, whereas equiaxed structures result from low-stress and high-temperature application, characteristic of creep.

3 RELEVANT DISLOCATION PROCESSES FOR CELL FORMATION

Dislocations exist in three dimensions inside a crystal. Since dislocations observed under experimental conditions are usually segments of complete dislocations, the character of such dislocations is usually determinable. However, the character of one segment doesn't necessarily determine the character of the entire dislocation. In addition, in a crystal with different slip systems, different parts of the same dislocation may be moving on different planes at the same time.

Dislocations can therefore be considered 'links' of screw, edge and mixed character operating on the slip systems. If the dislocations move on the primary slip system they are termed 'primary dislocations', and if they operate on others they are called 'secondary dislocations'. The primary dislocations are usually the first to exhibit motion of any kind upon deformation. After a critical value of applied stress and temperature, the secondary dislocations are activated and begin to interact with the primary dislocations, leading to multiplication and other processes.

Mobile dislocations are those that respond to applied stress by moving through the crystal, and subsequent creeping of the material is usually attributed to this motion.[5] Immobile dislocations are stationary in the material, and are responsible for dislocation multiplication by providing pinning points for mobile dislocations. In addition, they act as anchor points for dislocation accumulation, possibly providing a fixed source of inhomogeneity which ultimately leads to cell formation. It is found that the immobile dislocation density increases with temperature[18] and progressive straining of the material.[19]

When dislocations begin to cluster inside the matrix, they can combine to form dislocation dipoles and multipole bundles. A dipole is a group of two dislocations of the same character but opposite Burgers vector sign, which are close enough to be trapped but not close enough to annihilate. A multipole is a collection of more than two dislocations in a stable configuration. In the following, we briefly describe dislocation processes that contribute to cell formation.

3.1 Glide

During steady-state creep the production of dislocations usually results from the gliding of dislocations along preferred crystallographic directions, and which ultimately reproduce through the Frank–Read process. At lower temperatures, obstacles controlling glide are overcome by stress-assisted thermal activation. At intermediate temperatures, it has been suggested that obstacles controlling glide are athermal,[20] causing the flow stress to be approximately constant with temperature at higher temperatures. Assuming that the average spacing of obstacles in the matrix is λ, the glide velocity is given[21] by

$$v_g = M_g b^2[\sigma_a - (Gb/\lambda)] \tag{1}$$

where M_g is the glide mobility, b is the Burgers vector, σ_a is the applied stress, and G is the shear modulus.

The process of glide is limited by the mobility of the dislocation along the plane on which it is gliding. A general form of this mobility is given by the following expression:[22]

$$M_g = D_s b/kT \tag{2}$$

where D_s is the self-diffusion coefficient.

When the primary mode of dislocation motion is governed by the propagation of kinks through the matrix, the mobility is given[23] by

$$M_g = 2(h^2/a_0 b_0)(D_k/kT)\exp(-F_k/kT) \tag{3}$$

where h is the kink height, a_0 and b_0 are characteristic crystallographic dimensions, D_k is the kink diffusivity, and F_k is the kink formation energy.

3.2 Climb

At higher temperatures this phenomenon becomes a more dominant mode of dislocation motion, and since the formation of cellular structures occurs at higher temperatures the two processes may be uniquely coupled. Climb, however, is not necessarily a 'critical' phenomenon. In fact at lower temperatures climb still occurs at much lower velocities. A compilation of several expression for climb velocity[24–28] leads to the following expression:

$$v_c = \frac{A\sigma\Omega D_v}{bkT} c_j(\xi/\mu b)^2 \tag{4}$$

where σ is the normal stress acting across dislocation half plane, D_v is

the vacancy diffusion coefficient, c_j is the concentration of jogs, ξ is the stacking fault energy, and $A = 2(24\pi(1-\nu)/(2+\nu))^2$.

If we write the climb velocity $v_c = M_c b\sigma$, then the mobility of dislocation climb M_c is given by

$$M_c = A\left[\frac{D_v}{b}\right]\left[\frac{\mu\Omega}{kT}\right]c_j\left[\frac{\xi}{\mu b}\right]^3\frac{1}{\xi} \tag{5}$$

3.3 Multiplication

Dislocation multiplication is attributed to either the Frank–Read or the Bardeen-Herring sources. During dislocation creep, the Frank–Read source is dominant and multiplication occurs by pinning of the dislocation, bowing out, and wrapping around the pinning points.[29] Caillard and Martin[5] have identified these points in aluminum as primarily small precipitates or impurity clusters, and to some degree junction segments produced by two dislocations.[30] The latter mechanism is ruled out by the aforementioned authors as a major source, because the stress necessary to activate sources from these points is usually high enough to cause junction recombination.[31] On the other hand, Prinz and Argon[32] have identified anchoring points as dislocation dipoles and multipole bundles in the evolution of cell wall type structures.[33,34] The bowing out of free segments from these bundles is considered a major source generation.[32]

Dislocation multiplication is also possible through a climb process similar to the Frank–Read source, known as the Bardeen–Herring mechanism.[35] The contribution to production due to the bowing of dislocation links by climb has been calculated by Nabarro.[36] It has been determined, however, that this contribution is usually negligible compared to the recovery creep component[37] and is therefore not a major source of production of new dislocations.

3.4 Annihilation

Annihilation of dislocations of opposite Burgers vectors has usually been treated as an average over the crystal of the recovery process.[38,39] Essmann and Muhgrabi[40] have estimated a value of the critical distance for annihilation of two screw dislocations of opposite Burgers vector. This distance is

$$y_s = \frac{Gb}{2\pi\tau} \tag{6}$$

where τ is the stress required for dislocation glide.

It was found that for copper, an fcc metal, $y_s \simeq 1{\cdot}8\,\mu m$. For molybdenum, a bcc metal, $y_s \simeq 0{\cdot}19\text{–}2{\cdot}25\,\mu m$. For mixed or edge dislocations it is found that annihilation will occur when the attractive elastic force between two dislocations exceeds the force required for dislocation climb.[41] The critical distance for annihilation of mixed dislocations is thus given by

$$y_m = \frac{Gb^4}{2\pi K U_f \sin \psi} \tag{7}$$

where U_f is the energy of formation of atomic defects, ψ is the angle between Burgers vector and dislocation line vector, and $1 - \nu < K < \nu$, where ν is Poisson's ratio.

Essmann and Rapp[42] have found that the critical distance for edge dislocation annihilation in copper is of the order of 1·6 nm; much smaller than the critical distance for screw dislocations. Prinz and coworkers[27] determined this number to be greater than 1·6 nm, but these experiments were carried out at higher temperatures.

3.5 Dipole formation

Above the critical distance for annihilation, two dislocations can form dipole configurations. Dipoles are composed of edge dislocations of opposite sign, and typical dipole lengths are of the order of tenths of microns.[40] Several experiments indicate the presence of these dipoles in preformed subgrain walls.[32,43] In fact the dipoles are important for providing anchoring points for dislocation accumulation in the formation of the wall structures.[33] In addition, the interaction of singular dislocations with dipoles (and multipoles) has been found to be an important reaction in the mechanism of strain hardening.[44,45]

3.6 Advanced dislocation processes

There are other mechanisms, which are more involved than those described above and contribute to the evolution of the dislocation cell structure. Sandstrom has summed up most of these reactions in two papers of particular interest.[22,46] Together with original work by Li,[47] these references describe which processes can contribute to dislocation cell and subgrain evolution after cell formation. Dislocation recovery can be described as four possible processes:[22]

(1) annihilation of dislocations within the cell,
(2) annihilation of dislocations in the cell boundary,
(3) absorption of dislocations close to the cell boundary,
(4) emission of dislocations from the cell boundary.

More recently, Ghoniem and coworkers[48] have proposed a mechanistic creep formulation which takes into account different dislocation species: mobile, immobile and boundary.

3.7 Recovery

Recovery occurs when the material is heated below the critical temperature for recrystallization (approximately $\frac{2}{3}T_m$).[3] The recovery process happens in several stages.[27,49] In the first two stages (termed stage II and stage III), point defects anneal out. In the third stage (stage IV), dislocation motion is well activated and rearrangement occurs. Some dislocations are swept out by groups of other dislocations, and some annihilation occurs. In this last stage, cells and subgrains are most likely to form.[50]

Although annihilation of dislocations is the primary mechanism of recovery once cells have formed, other mechanisms can occur which also contribute to recovery. Three types of recovery have been identified in reference to cellular structures:[5]

(1) subgrain coalescence by migration,
(2) dislocation annihilation by glide and cross-slip in mixed subboundaries, or *dynamic recovery,*
(3) reduction of mesh distortion by short distance climb, or *static recovery.*

Polygonization, the tendency for dislocations to achieve a lower energy configuration by aligning into regular substructures, is usually associated with recovery processes in cellular type configurations. It has been found[50] that materials with a lower stacking fault energy do not polygonize readily. Table 1 is a compilation of some fcc and bcc metals

TABLE 1
Comparison of Subgrain Sizes in Metals and Alloys during Creep Tensile Tests (from McElroy and Szkopiak[51])

Crystal structure	*Material*	*Stacking fault energy* (J/m^2)	*Subgrain size* (μm)
bcc	Iron	0·2	4–12
bcc	Fe/Si	0·2	2–20
fcc	Aluminum	0·2	10–100
fcc	Nickel	0·12	10–20
fcc	Copper	0·05	5–10
fcc	Stainless steel	0·015	2–7

which do exhibit a cellular structure formation under specific conditions.[51] It is seen that a material of a higher stacking fault energy is more likely to form subgrains, considering that the polygonization process is more difficult for materials in which subgrains of lower radius tend to nucleate.

Recovery and recrystallization are competing processes for removal of dislocations from the lattice.[52] It appears that, if a sufficient number of dislocations are produced, the material is capable of being reformed into a new set of grains. This is characteristic of materials of low stacking fault energy, in which production of dislocations is facilitated and recrystallization is more likely to occur. High strains and high temperatures accelerate the dislocation multiplication process.[53] Hence, under conditions like hot working, dynamic recrystallization can be a dominant mechanism provided the material has favorable lattice structure.

Materials with higher stacking fault energy favor dynamic recovery, in which the dislocations rearrange to relieve the strain or the work-hardened material. The dislocations tend to form subgrains, instead of grouping in larger masses to restructure the grains of the material. Grain boundary migration, which is responsible for sweeping out dislocations to form a new matrix in recrystallization processes, is less likely to occur in materials in which a well developed mobile subgrain structure has formed. Recovery is a more dominant mechanism at lower strains. In addition, higher temperatures increase dislocation mobility, and the net result of this is a clustering of dislocations within the grain. Therefore under conditions like high-temperature creep, dynamic recovery can be a dominant mechanism provided the material has a favorable lattice structure.

4 DISLOCATION PROCESSES DURING DEFORMATION

The dominant character of dislocations in the material changes throughout the deformation process. Initially, there exist in the matrix dislocations which, when activated by applied stress and temperature, move by gliding on primary slip systems. At low temperatures, the dislocations exhibiting motion are primarily of the edge type. Screw dislocations are able to annihilate due to stress-induced cross-slip.[54] This is true even in weakly deformed fcc crystals[55,56] and in other crystal configurations as well.[57,58] These dislocations will annihilate only if they are close enough for cross-slip to be effective. However, there is not a complete deficit of screw dislocations at low-temperature/low-stress

deformation, and the previous conditions must be satisfied for complete removal of screw dislocations.

Through level I deformation at low temperatures ('level' refers to level of strain, 'stage' to level of temperature), it is therefore found that most of the dislocations contributing to the deformation process are edge type. At low temperatures, climb is not significant[40] and therefore edge dislocations cannot annihilate by this process. In addition, two edge dislocations of opposite sign cannot annihilate mutually by glide. Edge dislocations not only begin to diffuse with applied stress and temperature, but combine to form edge dipoles. Screw dipoles which may form are most likely annihilated by cross-slip.

In level I to level II deformation at high temperatures, the dislocations have formed cell-like structures, and the walls of the cells are composed of edge dislocations, screw dislocations and mixed character dislocations. Once the cells have formed, whatever dislocations exist in the cells annihilate upon further increase in temperature during application of stress until only low-angle tilt boundaries exist within the material. Until the condensation of cell walls to subgrains occurs, the dislocations that exist in the walls are still able to be activated to become mobile dislocations. However, the population of true mobile dislocations, those existing well within the subgrain, is still rather low. Further deformation causes static recovery of cell walls, and movement of dislocations from cell walls through the interior of cells and even through other walls.

In materials where only single slip systems operate, the cell structure formed is usually anisotropic, with the dislocations in the cells being mostly edge type in character.[27] In materials in which many slip systems operate, the cells produced are more equiaxed and the dislocations in the walls are mixed in character.[2] Dislocations of one type or another constitute the cell walls of materials of different nature. For example, in molybdenum, a bcc metal, dislocations in the cell walls are of the edge type,[10] whereas in copper, an fcc metal, the same dislocations are of the screw type.[59]

In an extensive study of dislocations in aluminum at intermediate temperatures,[60] it was found that two or three of six possible Burgers vectors are present in the sub-boundaries. Most of these dislocations in the sub-boundaries are indeed of mixed character, with three coplanar Burgers vectors. It was also found that the dislocation segments in the network are close to glide planes. This is apparently true because dislocation cells represent a low-energy configuration of glide dislocations.[61]

Dislocation processes leading to the formation of cells and other

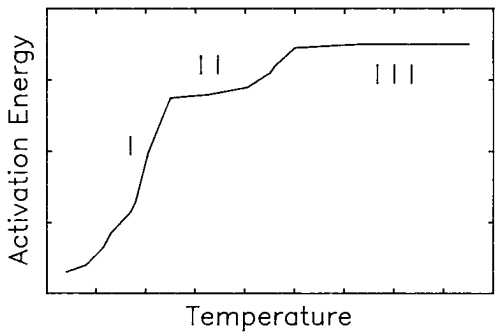

Fig. 3. Schematic of activation energy of aluminum vs temperature (from Dorn and Jaffe[62]).

structures in the matrix have been explained by many models in the literature. This has led to a separation into several schools on the dominant mechanism controlling steady-state dislocation creep.[2] Dorn has indicated that the dependence of creep on temperature occurs in three stages, corresponding to activation energies of the creep process.[62] This can be seen in Fig. 3 which shows the activation energy of creep of aluminum as a function of temperature. Caillard and Martin[4] have summarized the processes believed to be responsible for these different stages as follows.

4.1 Low-temperature deformation

At low temperatures, corresponding to the first energy plateau, they suggest that creep is governed by jog formation at the intersection of nonattractive dislocation junctions.[31] Muhgrabi has described in more detail this development of dislocation substructure at lower temperatures in several metals.[63] In particular, single-phase fcc metals such as copper were studied in tensile and cyclic conditions of deformation. In level I deformation, it was found that primary dislocations interact to form dipoles of mostly edge type. In level II deformation, secondary dislocations that have formed at the head of primary multipole bundles interact with the primary dislocations. Eventually, after the dislocation structures set, further deformation results in shrinkage of all characteristics of the substructure: dislocation spacings, segment length and the internal stress wavelength.

For deformation at lower temperatures, recovery processes involving self-diffusion are negligible. The mobility of screw dislocations is lower than that for an edge dislocation at low temperatures. Therefore, clustering of dislocations occurs primarily with edge dislocations, and

screw dislocations that are close enough to each other exhibit static recovery by cross-slip.[40] The resulting dislocation structures produce a long-range internal stress characteristic of multipolar configurations. This ultimately leads to minor coarsening of this bundle-oriented structure.

4.2 Intermediate and higher temperature deformation

At intermediate temperatures, the second plateau in energy (Fig. 3) is due to dislocation climb. In the region from the second plateau to the third energy plateau, the creep rate has been attributed to either of the two following processes:

(1) climb by pipe diffusion,[31,64–69]
(2) cross-slip.[5,62,70–72]

The processes discussed in this range for aluminum occur roughly above the temperature $0{\cdot}5T_m$, where dislocation cell formation is proposed to occur. For other materials,[4,27] the temperatures are in the range of $0{\cdot}3T_m$–$0{\cdot}5T_m$ for initial cell formation. As the temperature is raised further, cells condense into subgrains. According to Morris and Martin,[43] even though steady-state creep is occurring, the evolution of the cell structure is far from being at equilibrium. During an increase from intermediate to higher temperatures, the walls of cells not only condense to become low-angle subgrain walls, but grow and shrink in radius at the expense of other cells.

5 SUBGRAIN BOUNDARIES

5.1 Types of sub-boundary

Even though an ideal subgrain contains a boundary of single dislocations, the transition from cells to subgrains may actually occur when the boundary cross-section is reduced to a critical value of a few dislocations thickness. In fact, three types of sub-boundary have been identified in aluminum.[60] They are:

(1) symmetrical tilt boundaries,
(2) sub-boundaries with two orthogonal Burgers vectors,
(3) sub-boundaries with three coplanar Burgers vectors.

5.2 Internal stress

In level I deformation, the curvature of dislocations follows the applied stress. In level II, after secondary slip systems are activated and clustering of dislocations occurs, the curvature of the dislocations follows an 'effective stress'. This stress is the difference between the applied stress and the internal stress characteristic of the dislocation structure. For low-temperature deformation and certain alloy types,[73] the internal stress is believed to be an inherent property of dislocation bundles and clusters. In these tangles, high stresses originate from strong elastic interactions between close dislocation segments.

It has recently been shown that internal stresses arise as result of flexing of low-angle subgrain walls under an applied stress.[26,43,74–78] It has been suggested[79] that the anelastic recovery determined from stress reduction tests represents the motion of dislocations driven by long-range internal back stresses. Further evidence[77] reveals that this back stress is low when the substructure is homogeneous, but is significant after subgrains have formed. In addition, it was found that upon application of stress in class I alloys, where minimal clustering occurs, no significant transients occur.[26] In class II alloys, however, transients exist upon first loading and then after subsequent stress changes. These transients are attributed to the presence of cellular structures and subgrains, which are prevalent in deformed class II alloys.

5.3 Misorientation

The misorientation between subgrain boundaries is suggested to be responsible for the long-range internal stresses present in subgrains.[26] Just before secondary creep, this misorientation increases with increasing strain until steady state is reached.[80–82] At steady state, the misorientation angle between subgrains becomes independent of stress and temperature and reaches a value of the order of 1° for most metals and alloys.[2,74] For different metals this angle is larger for materials with higher stacking fault energy,[83] i.e. those materials that have a higher tendency to form subgrains.

5.4 Deformation

It is known that the migration of sub-boundaries occurs by dislocation glide.[5,73] It has also been found that sub-boundary migration accounts for anywhere from 5% to 25% of the total strain.[26,32,73] During steady-state creep, the subgrain walls are more or less stabilized by

reactions with secondary dislocations, in the form of nodes and stacking fault dipoles.[32] At high strains, there is much of this dislocation 'debris' in the cell walls and hardly any between the walls.[32,82] Once the subgrains have formed, natural sources of new dislocations are rather low. For example, the rate is less than about one dislocation per subgrain for aluminum.[5] This has led to the conclusion that the majority of creep strain may be due to the glide and/or climb of dislocations within the subgrain.[5,26]

It has therefore been proposed that steady-state creep deformation is controlled by the breakage of dislocation links from the subgrain walls and propagation of those dislocations through the subgrain interior.[5,37,65,84] The strain rate is influenced by the proportion of boundaries able to achieve dislocation emission[82] and the breakage of links results from the applied stress to the material.

6 THEORETICAL AND COMPUTATIONAL MODELS OF DISLOCATION CELL FORMATION

Around the turn of the century, Gibbs first proposed a hypothesis that stable states are achievable through minimization of the free energy of the system in consideration.[85] Cahn, many years later, was the first to utilize the principles set forth by Gibbs, and he developed much work related to spinodal decomposition.[86] More recently, Heerman[87] has done extensive work in presenting an updated critique and analysis of spinodal decomposition and related topics. His work also includes a description of computer simulation of phase transitions.

The application of these techniques has been limited to the description of chemical rate processes. Holt adapted these principles to the phenomenon of dislocation cell formation.[88] Using analysis similar to spinodal decomposition, he showed that an array of dislocations is inherently unstable to small perturbations. It was found that the dislocations moved to form a periodic structure of wavelength λ, characteristic of the diameter of the dislocation cell, which is given by the following equation:

$$\lambda \simeq K_c \rho^{-1/2} \tag{8}$$

where K_c is the constant of proportionality, and ρ is the average dislocation density.

The principle of minimizing the free energy to arrive at a stable configuration of the system was also used in an approach by Gittus[89–93] to determine the theoretical value of the constant K_c for metals.

Compilation of experimental evidence[2] reveals that, for metals, the value of K_c is of the order of 10. In other theoretical descriptions, Lagneborg and coworkers utilized a statistical approach[19,20,38,39,94] to determine the distribution of mobile dislocation links in materials upon application of stress. Argon and coworkers[2,24–28] investigated the effect of dislocation coarsening due to climb of dislocations within subgrain walls, and derived a phenomenological expression for the strain rate in subgrain forming metals.

Sandstrom[22,46] and Li[47] developed a set of kinetic equations based on fundamental dislocation reaction processes occurring within the cell and at the cell boundaries. In his formulation, Sandstrom utilized cell growth processes originally developed by Hillert[95] and Kocks[96] to describe the coarsening of cell-like structures. Other rate theory descriptions of the physics of dislocation substructure formation and dislocation interactions include the kinetics of interstitial and vacancy interaction with dislocations and dislocation loops.[97–99] A more recent model utilizing a rate theory description was developed by Ghoniem *et al.*[48] In this formulation, the evolution of the average dislocation density in high strength steel is coupled with a phenomenological theory of dislocation creep.

Nicolis and Prigogine[100] developed a theory describing self-organization of dissipative structures. Walgraef and Aifantis[101–104] utilized these concepts of self-organization to arrive at a description of the formation and stability of dislocation patterns in one, two and three dimensions. In their formulation they considered two species of dislocations, mobile and immobile, and developed a set of reaction–diffusion equations up to third-order nonlinearities. It was found that the competition between diffusive-like mobilities and cubic nonlinearities leads to stable periodic dislocation structures. These nonlinearities are attributed to the interaction of singular dislocations with dislocation dipoles, which are present in cyclically deformed metals having the tendency to form banded structures.

It is interesting to note the differences in approach by Holt and Walgraef and Aifantis. In Holt's formulation, the principle of minimization of free energy of the dislocation system is the chief driving force for the formation of periodic substructures. This methodology, however, is only applicable to the initial perturbed state of the dislocation system, and is not extendable to the entire sequence of pattern formation. The approach of Walgraef and Aifantis, however, is based upon interaction of dislocation species and the diffusion of the species through the medium. The principles of bifurcation are ap-

plicable here, and stable states are not produced by achievement of a minimum free energy, but by interplay between reaction elements and diffusive elements of the system.

In computational formulations, Gibeling and Nix[76] utilized principles of molecular dynamics to study the behavior of a dislocation sub-boundary, and an array of sub-boundaries. Gerberich *et al.*[105] utilized methods similar to the previous authors to study dislocation substructures and fatigue crack growth. They derived a computer model which simulated dislocation pile-ups, slip-band formation, and the interaction of dislocations with an idealized cell network. Other computational work includes simulation of dislocation motion,[106] dislocation production and recovery,[107] the effect of stress and temperature on high-temperature creep,[108,109] and the numerical simulation of persistent slip-band formation.[110]

A general methodology for application of computational statistics to physical systems was recently covered in an article by Abraham.[111] It has been found that, in dislocation systems, describing the characteristics of cellular pattern formation through application of accurate analytical treatments is difficult. This is a problem characteristic of nonlinear physical systems, and it was therefore suggested by Abraham that 'computer experiments' be designed to bridge the gap between theory and experiment. A methodology utilizing principles of computational statistical mechanics applied to two-dimensional cellular pattern formation was therefore recently proposed by Amodeo and Ghoniem.[112] The ability of this formulation to depict accurately the

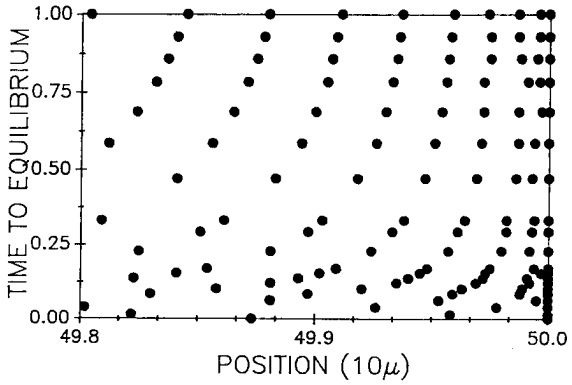

Fig. 4. Time evolution of a 1-D 50 dislocation pile-up (from Amodeo and Ghoniem[112]).

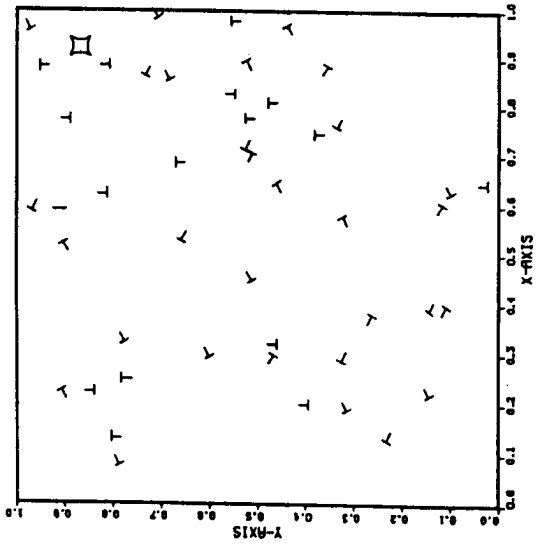

it# = 18 , t = 1.89 x 10^4 s

(a)

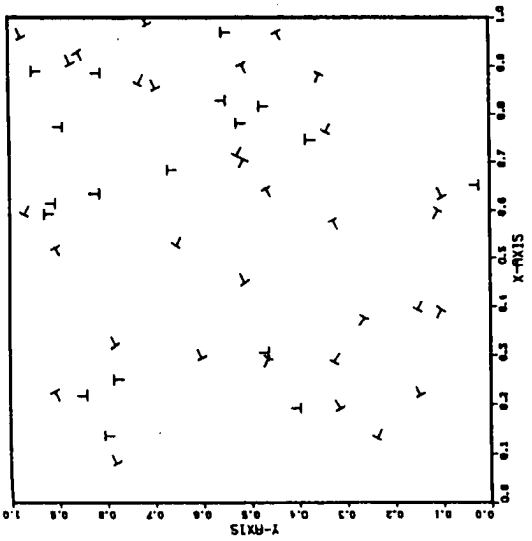

it# = 0 , t = 0 s

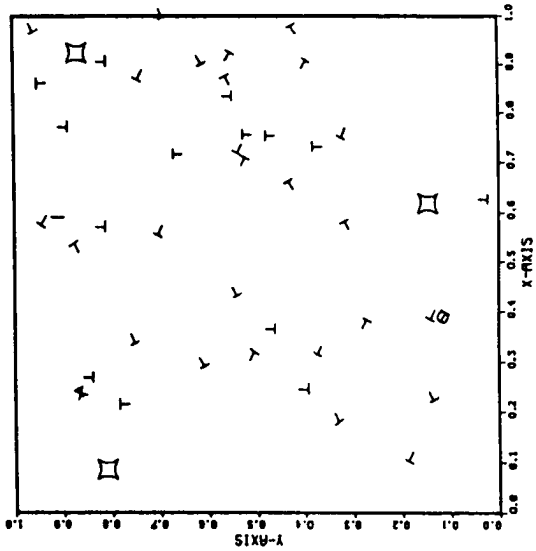

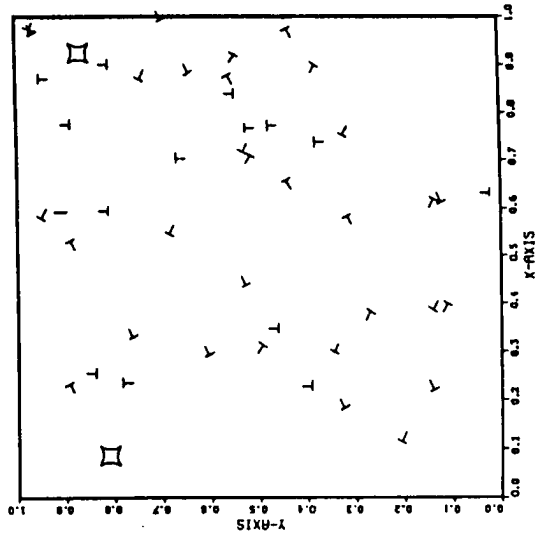

(b)

Fig. 5. Two-dimensional dislocation simulation sequence.

phenomenon of cell formation can be represented by the following characteristics:

(1) the inclusion of grain boundary effects,
(2) the inclusion of dislocations with multiple Burgers vectors which are capable of operating on multiple slip systems,
(3) the potential for dislocation clustering and multiple dislocation interactions,
(4) an insight into the physical mechanisms responsible for the formation of cellular structures by application of more fundamental physical principles.

The basic numerical procedure employed in a molecular dynamics simulation is the solution of the equation of motion by an explicit central difference formula.[113] Applied to dislocation systems, the position and velocity are given by the following equations, which are similar to the leapfrog equations used in plasma particle simulations:[114]

$$\mathbf{v}_i = M\mathbf{F}_{i-1} \tag{9}$$

$$\mathbf{r}_i = \mathbf{r}_{i-1} + \mathbf{v}_i \, \Delta t \tag{10}$$

$$\mathbf{F}_i = \mathbf{F}[\mathbf{r}_i] = (\mathbf{b} \cdot \boldsymbol{\sigma}[\mathbf{r}_i]) x \boldsymbol{\xi} \tag{11}$$

where $\mathbf{b}$ is the dislocation vector, $\boldsymbol{\xi}$ is the dislocation line vector, and $\boldsymbol{\sigma}$ is the stress tensor.

The current velocity is calculated from the current dislocation configuration, i.e. from the forces due to the fixed positions of the dislocations. The current positions are calculated based on the new dislocation configuration. The force $\mathbf{F}_i$ in eqn (11) is calculated using continuum mechanics for solid materials, and is proportional to $1/r$, where r is the radial distance from the dislocations.

The timestep chosen for the system is the minimum amount of time it would take two dislocations to experience a reaction, whether it be collision or annihilation. If we consider two dislocations of arbitrary Burgers vectors coming in close vicinity to one another, this timestep can be expressed by the following condition:

$$\Delta t = \min (\Delta r_{ij} / \Delta v_{ij}) \tag{12}$$

where

$$\Delta r_{ij} = |r_i - r_j| \tag{13}$$

$$\Delta v_{ij} = |v_i - v_j| \tag{14}$$

Results from a simulation of a one-dimensional pile-up of 50 dislocations can be seen in Fig. 4, which displays the dynamics of the

first few of the 50 dislocations encountering an obstacle on the right vertical axis.

Figure 5 is a two dimensional transgression in time of the simulation of motion of 50 dislocations of six different Burgers vectors, for a condition of zero applied stress. The first frame is the initial condition of the crystal, with dislocations strewn randomly through the matrix. The following frames are a demonstration of several processes which occur over a period of time of natural evolution. In particular, dipole formation (represented by a straight line), junction immobilization (represented by a box), and dislocation immobilization (represented by a circled dislocation) are three interactive processes characterized in this simulation. Further results of the simulation in one and two dimensions are currently being investigated.

ACKNOWLEDGEMENTS

This work was supported by the US Department of Energy, Office of Fusion Energy, Grant No. DE-FG03-84ER52110, with UCLA.

REFERENCES

1. Miekk-oja, H. M. and Lindroos, V. K., in *Constitutive Equations in Plasticity,* Argon, A. S. (ed.), MIT Press, Massachusetts, 1935, p. 327.
2. Takeuchi, S. and Argon, A. S., *J. Mat. Sci.,* **11** (1976) 1542.
3. Jonas, J. J., Sellars, C. M. and Tegart, W. J. McG, *Metall. Rev.,* **14** (1969) 1.
4. Caillard, D. and Martin, J. L., *Acta Met.,* **30** (1982) 437.
5. Caillard, D. and Martin, J. L., *Acta Met.,* **31** (1983) 813.
6. Garofalo, F., Zwell, L., Keh, A. S. and Weissmann, S., *Acta. Met.,* **9** (1961) 721.
7. Lytton, J. L., Barrett, C. R. and Sherby, O. D., *Trans. Met. Soc. AIME,* **233** (1965) 1399.
8. Gupta, V. P. and Strutt, P. R., *Canad. J. Phys.,* **45** (1967) 1213.
9. Jones, B. L. and Sellars, C. M., *Metal Sci. J.,* **4** (1970) 96.
10. Clauer, A. H., Wilcox, B. A. and Hirth, J. P., *Acta Met.,* **18** (1970) 381.
11. Poirier, J. P., *Phil. Mag.,* **26** (1972) 713.
12. Huther, W. and Reppich, B., *Phil. Mag.,* **28** (1973) 363.
13. Streb, G. and Reppich, B., *Phys. Stat. Sol.* (*a*) **16** (1973) 493.
14. Reppich, B., *J. Mat. Sci.,* **6** (1971) 267.
15. Hasegawa, T., Hasegawa, R. and Karashima, S., *Trans. Jap. Inst. Metals,* **11** (1970) 101.
16. Orlova, A., Pahutova, M. and Cadek, J., *Phil. Mag.,* **25** (1972) 865.
17. Sherby, O. D. and Burke, P. M., *Prog. Mat. Sci.,* **13** (1967) 325.

18. Nohara, A., *Phys. Stat. Sol (a)*, **88** (1985) 213.
19. Lagneborg, R. and Forsen, B. H., *Acta Met.*, **21** (1973) 781.
20. Ostrom, P. and Lagneborg, R., *J. Eng. Mat. Tech. Trans. ASME, Ser. H.*, **98** (1976) 114.
21. Burton, B., *Phil. Mag. A*, **51** (1985) L13.
22. Sandstrom, R., *Acta Met.*, **25** (1977) 905.
23. Hirth, J. P. and Lothe, J., *Theory of Dislocations*, Wiley-Interscience, New York, 1982.
24. Takeuchi, S. and Argon, A. S., *Acta Met.*, **24** (1976) 883.
25. Argon, A. S. and Moffatt, W. C., *Acta Met.*, **29** (1981) 293.
26. Argon, A. S. and Takeuchi, S., *Acta Met.*, **29** (1981) 1877.
27. Prinz, F., Argon, A. S. and Moffatt, W. C., *Acta Met.*, **30** (1982) 821.
28. Burton, B., *Phil. Mag. A*, **46** (1982) 607.
29. Read, W. T., *Dislocations in Crystals*, McGraw-Hill, New York, 1953.
30. Caillard, D. and Martin, J. L., in *Creep and Fracture of Engineering and Structures*, Wilshier, B. and Owen, D. R. J. (eds), Pineridge Press, Swansea, 1981, p. 17.
31. Saada, G., *Acta Met.*, **8** (1960) 841.
32. Prinz, F. and Argon, A. S., *Phys. Stat. Sol. (a)*, **57** (1980) 741.
33. Muhgrabi, H., *Phil. Mag.*, **23** (1971) 897.
34. Argon, A. S., in *Physics of Strength and Plasticity*, Argon, A. S. (ed.), MIT Press, Cambridge, 1970, p. 217.
35. Bardeen, J. and Herring, C., *Imperfections in Nearly Perfect Crystals*, Wiley, New York, 1952.
36. Nabarro, F. R. N., *Phil. Mag. A*, **16** (1967) 231.
37. Burton, B., *Phil. Mag. A*, **45** (1982) 657.
38. Lagneborg, R., *Met. Sci. J.*, **3** (1961) 161.
39. Lagneborg, R., *Met. Sci. J.*, **6** (1972) 127.
40. Essmann, U. and Muhgrabi, H., *Phil. Mag.*, **40** (1979) 731.
41. Friedel, J., *Dislocations*, Pergamon Press, Oxford, 1954.
42. Essmann, U. and Rapp, M., *Acta Met.*, **21** (1973) 1305.
43. Morris, M. A. and Martin, J. L., *Acta Met.*, **32** (1984) 549.
44. Chen, H. S., Gilman, J. J. and Head, A. K., *J. Appl. Phys.*, **35** (1964) 2502.
45. Neumann, P. D., *Acta Met.*, **19** (1971) 1233.
46. Sandstrom, R., *Acta Met.*, **25** (1977) 897.
47. Li, J. C. M., *J. Appl. Phys.*, **33** (1962) 2958.
48. Ghoniem, N. M., Matthews, J. R. and Amodeo, R. J., *A dislocation model for creep in engineering materials*, AERE Harwell Report No. TP1224, February, 1987.
49. Van den Beukel, A., in *Vacancies and Interstitials*, Seeger, A., Schumacher, D., Schilling, W. and Deihl, J. (eds), North-Holland, Amsterdam, 1970, p. 427.
50. Hardwick, D. and Tegart, W. J. McG., *J. Inst. Metals*, **90** (1961) 17.
51. McElroy, R. J. and Szkopiak, Z. C., *Int. Met. Rev.*, **17** (1972) 175.
52. Sandstrom, R. and Lagneborg, R., *Acta Met.*, **23** (1975) 387.
53. Sakai, T. and Jonas, J. J., *Acta Met.*, **32** (1984) 189.
54. Essmann, U., *Acta Met.*, **12** (1984) 1468.
55. Fourie, J. T. and Murphy, R. J., *Phil. Mag. A*, **7** (1962) 1617.

56. Mader, S., Seeger, A. and Theiringer, H. M., *J. Appl. Phys.*, **34** (1963) 3376.
57. Hirsch, P. B. and Lally, J., *Phil. Mag.*, **12** (1965) 595.
58. Taylor, G. and Christian, J. W., *Phil. Mag.*, **15** (1967) 893.
59. Hasegawa, T. and Karashima, S., *Met. Trans.*, **1** (1970) 1052.
60. Caillard, D. and Martin, J. L., *Acta Met.*, **30** (1982) 791.
61. Kuhlmann-Wilsdorf, D. and Van der Merwe, J. H., *Mat. Sci. Eng.*, **55** (1982) 79.
62. Dorn, J. E. and Jaffe, N., *Trans. Met. Soc. AIME,* **221** (1961) 229.
63. Muhgrabi, H., in *Constitutive Equations in Plasticity,* Argon, A. S. (ed.), MIT Press, Massachusetts, 1935, p. 327.
64. Luthy, H., Miller, A. K. and Sherby, O. D., *Acta Met.*, **28** (1980) 169.
65. Evans, H. E. and Knowles, G., *Acta Met.*, **25** (1977) 963.
66. Sherby, O. D. and Weertman, J., *Acta Met.*, **27** (1979) 387.
67. Barrett, D. R. and Nix, W. D., *Acta Met.*, **13** (1965) 1247.
68. Spingarn, J. R., Barnett, D. M. and Nix, W. D., *Acta Met.*, **27** (1978) 1549.
69. Turunen, M. J., *Acta Met.*, **24** (1976) 463.
70. Friedel, J., *Rev. Phys. Appl.*, **12** (1977) 1649.
71. Poirier, J. P., *Rev. Phys. Appl.*, **11** (1976) 731.
72. Schoeck, G., *Creep and Recovery,* Am. Soc. Metals, Cleveland, 1956, p. 199.
73. Caillard, D., *Phil. Mag. A,* **51** (1985) 157.
74. Exell, S. F. and Warrington, D. H., *Phil. Mag. A,* **26** (1972) 1121.
75. Muhgrabi, H., *Acta Met.*, **31** (1983) 1367.
76. Gibeling, J. C. and Nix, W. P., *Acta Met.*, **28** (1980) 1743.
77. Hasegawa, T., Ikeuchi, Y. and Karashima, S., *Met. Sci. J.*, **6** (1972) 78.
78. Hirth, J. P., *Met. Trans.*, **3** (1972) 3047.
79. Gibeling, J. C. and Nix, W. P., *Acta Met.*, **29** (1981) 1769.
80. Morris, M., Masson, D., Senior, B. and Martin, J. L., *Scripta Met.*, **17** (1983) 6871.
81. Suh, S. H., Cohen, J. B. and Weertman, J., *Met. Trans. A,* **14** (1983) 117.
82. Morris, M. A. and Martin, J. L., *Acta Met.*, **32** (1984) 1609.
83. Kozyrskiy, G. Ya., Okrainets, P. N. and Pischchah, V. K., *Phys. Met. Metallogr.*, **34** (1972) 151.
84. Schwink, C. and Gottler, E., *Acta Met.*, **24** (1976) 173.
85. Gibbs, J. W., *Collected Works,* vol. **1**, pp. 105–115, 252–258, Yale University Press, New Haven, Connecticut, 1948.
86. Cahn, J. W., *Acta Met.*, **9** (1961) 795.
87. Heerman, D. W., *Phys. Rev. Lett.*, **52** (1984) 1126.
88. Holt, D., *J. Appl. Phys.*, **41** (1970) 3197.
89. Gittus, J. H., *Acta Met.*, **22** (1974) 789.
90. Gittus, J. H., *Phil. Mag.*, **34** (1976) 401.
91. Gittus, J. H., *Phil. Mag.*, **35** (1977) 293.
92. Gittus, J. H., *Phil. Mag.*, **39** (1979) 829.
93. Gittus, J. H., *Phil. Mag.*, **35** (1981) 337.
94. Ostrom, P. and Lagneborg, R., *Res. Mechanica,* **1** (1980) 59.
95. Hillert, M., *Acta Met.*, **13** (1965) 227.